Talanta 127 (2014) 43–50

Contents lists available at ScienceDirect

Talanta

journal homepage: www.elsevier.com/locate/talanta

In situ tracking the intracellular delivery of antisense oligonucleotides by fluorescein doped silica nanoparticles

Peng Zhang [a], Tian-Yi Wang [b], Huan-Ming Xiong [b,*], Ji-Lie Kong [a,**]

[a] Department of Chemistry and Institutes of Biomedical Sciences, Fudan University, Shanghai 200433, China
[b] Department of Chemistry and Shanghai Key Laboratory of Molecular Catalysis and Innovative Materials, Fudan University, Shanghai 200433, China

ARTICLE INFO

Article history:
Received 17 January 2014
Received in revised form
15 March 2014
Accepted 18 March 2014
Available online 3 April 2014

Keywords:
Antisense oligonucleotides
Fluorescein doped silica nanoparticles
Confocal laser scanning microscopy
In situ tracking

ABSTRACT

Antisense oligonucleotides (ASOs) are often utilized to interfere with gene expression at mRNA level for cancer treatment. Here, we synthesized fluorescein doped silica nanoparticles (FSNPs) and coated them by polyethyleneimine (PEI) for carrying ASOs. Agarose gel electrophoresis proved that PEI/FSNPs could load ASOs by a weight ratio as high as 30:1. We tracked the delivery process of ASOs from the ASOs/PEI/FSNPs composites to HeLa cells in situ by the confocal laser scanning microscopy (CLSM) techniques, including nuclear staining and *Z*-axis scanning. We found the ASOs/PEI/FSNPs composites exhibited their biological effects at specific intracellular localization, and the fluorescence of the FSNPs showed the dynamic delivery process in the cells.

1. Introduction

Antisense oligonucleotides (ASOs) are short single-strand DNA chains with 12–25 nucleotides. They can inhibit gene expression through binding to the target mRNA [1–4]. Although ASOs have such a promising function in the field of cancer therapy, their poor stability toward nuclease and low intracellular uptake hinder their practical applications [5,6]. In the early researches, viral vectors were used for ASOs delivery, but the immunogenicity formed a barrier [7,8]. Later, polymer microspheres, liposome micelles [9–12], and nanocarriers were employed for gene delivery. Nanocarriers not only protected DNA against nuclease degradation but also helped DNA penetrate the cell membrane [13–15]. The common nanocarriers include gold nanoparticles [16–19], quantum dots [20–22], carbon nanotubes [23–27], etc. Among them, silica nanoparticles have received intensive attention due to their good stability and biocompatibility.

Organic dye doped silica nanoparticles with diameters of hundreds of nanometers were first synthesized by Vanblaaderen and Vrij [28,29] following the classical Stöber method [30]. Later, Tan's group [31–33] incorporated metallorganic dyes into the matrix of silica nanoparticles with diameter of tens of nanometers through the reverse microemulsion technique [34]. In comparison with the dyes dissolved in solutions, dye-doped silica nanoparticles exhibited more bright and more stable fluorescence [35]. These fluorescent silica nanoparticles were used for detecting nucleic acids [36,37] and imaging cells [38–40]. In order to make silica nanoparticles positively charged for carrying DNA, both organic silanes [41–43] and cationic polymers [44–48] were used to modify the silica surfaces. For example, in a polyethylene imine (PEI) involved delivery system, the proton sponge effect, which arises from the large number of amine groups on PEI and renders proton absorption in acidic organelles, induced endosomes' osmotic swelling and the rupture of the endosomal membrane [21,49–51].

Survivin protein often over-expresses in cancer cells, and plays an important role in the inhibition of apoptosis as well as the promotion of cell proliferation [52]. Therefore, silencing survivin protein's expression is helpful in cancer therapy. Peng et al. [53] once employed amino silica nanoparticles as carriers for survivin ASOs' transportation, but it was still unclear that how silica nanoparticles delivered ASOs into cells and where they exactly located in cells. Lately, Li et al. [54] used survivin ASOs tethered quantum dots (QDs) to regulate survivin mRNA successfully, while the cytotoxicity of the QDs remained a problem.

In the present work, we designed a carrier based on PEI modified fluorescein doped silica nanoparticles (FSNPs) to transport survivin ASOs into cancer cells, and in situ tracking the ASOs/PEI/FSNPs nanocomposites' delivery to HeLa cells for the first time (Fig. 1). The results showed that the PEI/FSNPs nanocomposites were biocompatible even at high dosage. After ASOs delivery, the survivin expression in HeLa cells was reduced successfully. A real time tracking experiment was conducted by a confocal laser scanning microscope (CLSM) to observe how the ASOs/PEI/FSNPs

* Corresponding author. Tel.: +86 21 65642138; fax: +86 21 65641740.
** Corresponding author. Tel.: +86 2155664397; fax: +86 21 65641740.
E-mail addresses: hmxiong@fudan.edu.cn (H.-M. Xiong), jlkong@fudan.edu.cn (J.-L. Kong).

http://dx.doi.org/10.1016/j.talanta.2014.03.045
0039-9140/

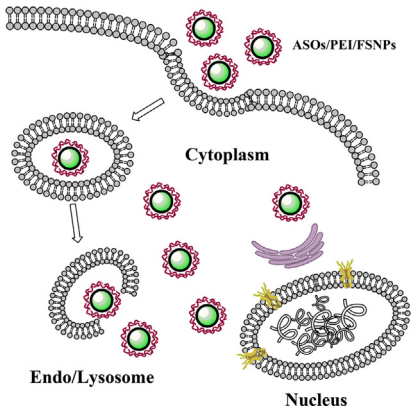

Fig. 1. Schematic representation of PEI modified fluorescein doped silica nanoparticles (FSNPs) as carriers to deliver antisense oligonucleotides (ASOs). The targeted survivn proteins' expressions are down-regulated by ASOs. Taking advantage of the PEI/FSNPs' fluorescence, in situ tracking the ASOs/PEI/FSNPs nanocomposites' delivery to HeLa cells is pursued.

nanocomposites entered and migrated in cells and where they located and functioned finally.

2. Experimental

2.1. Materials

Tetraethylorthosilicate (TEOS), aminopropyltriethoxysilane (APTES), fluorescein isothiocyanate (FITC), rhodamine B isothiocyanate (RBITC), polyethyleneimine (PEI, 25 kD) were purchased from Sigma-Aldrich (USA). Triton X-100 was purchased from Alfa Aesar China (Tianjin, China). Cyclohexane, *n*-hexanol, ethanol, 25% ammonium hydroxide were purchased from Sinopharm Chemical Reagent Co., Ltd. (Shanghai, China). 3-(4,5-dimethylthiazol-2-yl)-2,5-diphenyltetrazolium bromide (MTT) and antisense oligonucleotides (ASOs) were purchased from Sangon Biotechnology Co., Ltd. (Shanghai, China), Dulbecco's Modified Eagle's Medium (DMEM), Fetal calf serum (FCS) were purchased from GBICO. 2-(4-amidinophenyl)-6-indolecarbamidine dihydrochloride (DAPI) was purchased from KeyGen Biotech. (Nanjing, China). For all experiments and analyses, water was deionized. All chemicals were analytic grade and used without further purification. The antisense oligonucleotides (ASOs) sequences are listed in Table S1.

2.2. Synthesis and surface modification of FSNP

Before the synthesis, 1 mg of FITC was dissolved in 2.5 mL of *n*-hexanol under sonication, and then 10 μL of APTES was added, this reaction was continued for 24 h with magnetic stirring. Typically, FSNP were synthesized in the W/O microemulsion system. The microemulsion consisted of a mixture of Triton X-100 (10.6 mL), *n*-hexanol (9.6 mL), cyclohexane (45.0 mL), deionized water (3.5 mL), FITC-APTES solution (1.2 mL) and TEOS (0.6 mL) that was stirred for 30 min, and then 0.60 mL of ammonia hydroxide was added. After 24 h of stirring, the FSNP were isolated from the microemulsion with acetone. Several centrifugation and washing steps with ethanol and water were used to remove the surfactant and the impurities. The obtained FSNPs were kept in distilled water for use.

For surface modification, 10 mg of FSNP was added into 10 mL of PEI water solution (1 mg/mL). After the mixture was sonicated for 30 min, the PEI modified FSNP was washed by deionized water for three times.

To label PEI with rhodamine B, 60 mg of PEI was dissolved in 10 mL of carbonate buffer (pH 9) and mixed with 1 mL of DMSO containing 1 mg of rhodamine B isothiocyanate. The mixture was stirred for 24 h at room temperature and dialyzed against distilled water [55]. The rhodamine B-labeled PEI was attached to the FSNPs by using similar procedure as mentioned above.

2.3. DLS and ζ-potential

DLS experiments and ζ-potential measurements were carried out using a Malvern Zetasizer (Nano series, Malvern Instruments Inc., USA).

2.4. Thermogravimetric analyses (TGA)

Thermogravimetric analyses (TGA) were conducted on a Perkin Elmer instruments (TGA7) with a heating rate of 10 °C/min in an air flow.

2.5. Agarose retardation

40 μg of PEI/FSNPs were mixed with TAMAR-labeled antisense oligonucleotides at various weight ratios. After 30 min incubation, the electrophoretic mobility of the mixture was visualized on 1% (W/V) agarose gel under 365 nm excitation. The measurement was carried out for 30 min at 80 V in 1 × TBE buffer (44.5 mM Tris / HCl, 44.5 mM borate acid, 1 mM EDTA, pH 8.3).

2.6. Cell culture

Human cervical carcinoma (HeLa) cells were routinely cultured at 37 °C in flasks containing Dulbecco's Modified Eagle Medium (DMEM) with 10% fetal calf serum (FCS) in a humidified atmosphere and with 5% CO_2 in a Thermo culturist.

2.7. Cytotoxicity assay

PEI/FSNPs complexes' cytotoxicity was determined by MTT assay. HeLa cells were first seeded at 10^4 per cell into the 96-well cell culture plate in DMEM with 10% FCS at 37 °C and with 5% CO_2 for 24 h, then, different concentrations of PEI/FSNPs composites were added, after incubation for 24 h, MTT (100 μL, 5 mg/mL) was added and incubated for 4 h, at last, the formed formazan was dissolved in DMSO. The absorbance at 492 nm was recorded by an automatic ELISA analyzer (SPR-960).

2.8. Confocal laser scanning microscopy (CLSM) of subcellular localization of ASOs/PEI/FSNPs composites

HeLa cells were grown in Dulbecco's modified Eagle's medium (DMEM) supplemented with 10% fetal calf serum (FCS) at 37 °C and 5% CO_2. Cells were seeded on 15 mm glass bottom petridishes and allowed to adhere for 24 h. After 24 h of incubation, the cells were washed with PBS three times. Then, HeLa cells were incubated with ASOs/PEI/FSNPs composites in DMEM supplemented with 10% FBS at 37 °C under 5% CO_2. After incubation, the cells were fixed with 4% paraformaldehyde in PBS for 15 min at 37 °C, and stained with DAPI (0.2 μg/mL) in PBS for 20 min at 37 °C. Confocal fluorescence imaging was performed with a Leica laser scanning confocal microscope (Leica TCS SP5) under a 40 × objective lens. The excitation for DAPI was 405 nm, and the fluorescence emission was monitored from 430 nm to 450 nm. The excitation for FSNPs was 488 nm, and the fluorescence emission was monitored from 500 nm to 530 nm. The excitation for ASOs-TAMAR was 543 nm, and the fluorescence emission was monitored from 580 nm to 700 nm.

2.9. Real-time tracking of ASOs/PEI/FSNPs composites by CLSM

The whole experiment was performed by an in situ real-time confocal microscopy technique. The temperature was set at 37 °C and CO_2 was 5% (in volume). The observing time was 23 h, and the fluorescence images were collected automatically every 1 h. The excitation for FSNPs was 488 nm, and the fluorescence emission was monitored from 500 nm to 530 nm. The excitation for ASOs-TAMAR was 543 nm, and the fluorescence emission was monitored from 580 nm to 700 nm.

2.10. Flow cytometry (FCM)

After transfection, the cell culture medium was removed, and the cells were washed and detached from the plate by treating with 0.25% trypsin for 3 min at room temperature. Then, the cells were collected by centrifugation. The data presented here represent the mean fluorescence obtained from a population of 10,000 cells. Samples were analyzed on a Becton Dickinson FACS Calibur flow cytometer. The cell was excited at 488 nm and fluorescence was analyzed at 520 nm.

2.11. Western blots

Transfected cells were lysed and centrifuged. The supernatants were collected and the protein concentration was measured with a BCA protein assay kit. Equal amounts of protein were first loaded and separated by SDS-PAGE, and then transferred for 2 h at 200 mA to nitrocellulose membranes in transfer buffer and blocked with 5% milk blocking buffer overnight on a horizontal shaker. The blocked membranes were incubated with rabbit monoclonal Survivin antibodies (1:400, Cell Signaling Technology) diluted in 5% milk blocking buffer for 2 h. The membranes were washed in Tween-phosphate-buffered saline (TBST) and probed with horseradish peroxidase (HRP)-labeled goat anti-rabbit secondary antibody (1:10,000, Beijing Biosynthesis Biotechnology) in 5% milk blocking buffer. The membranes were exposed for data acquisition and developed using a conventional film-developing machine.

3. Results and discussion

3.1. Silica nanoparticles characterization

The size of the as-prepared FSNPs was around 50 nm, as seen by the transmission electron microscope (Fig. 2A and B). The hydrodynamic diameter of FSNPs in pure water was measured by dynamic light scattering (DLS), and showed an average diameter of 78 nm with relatively narrow distribution (polydispersity index (PDI)=0.126; Fig. 2C). The UV absorption and photoluminescence analyses proved the fluorescein had been doped into silica nanoparticles (Fig. S1). Since FITC was covalently linked to the silica matrix, no dye leaking was observed in an aqueous supernatant when FSNPs were centrifuged (Fig. S1). As we know, pure silica nanoparticles exhibit negative ζ-potential values around −50 mV. This was due to the presence of deprotonated silanol groups on the silica surface (pK_a=7.0) [38]. In our case, although the protonated amine groups (pK_a=9.0) usually reduced the ζ-potential value, but the amount of tetraethylorthosilicate (TEOS) employed in the synthesis was much larger than that of APTES, and thus the final FSNPs' ζ-potential was around −40 mV.

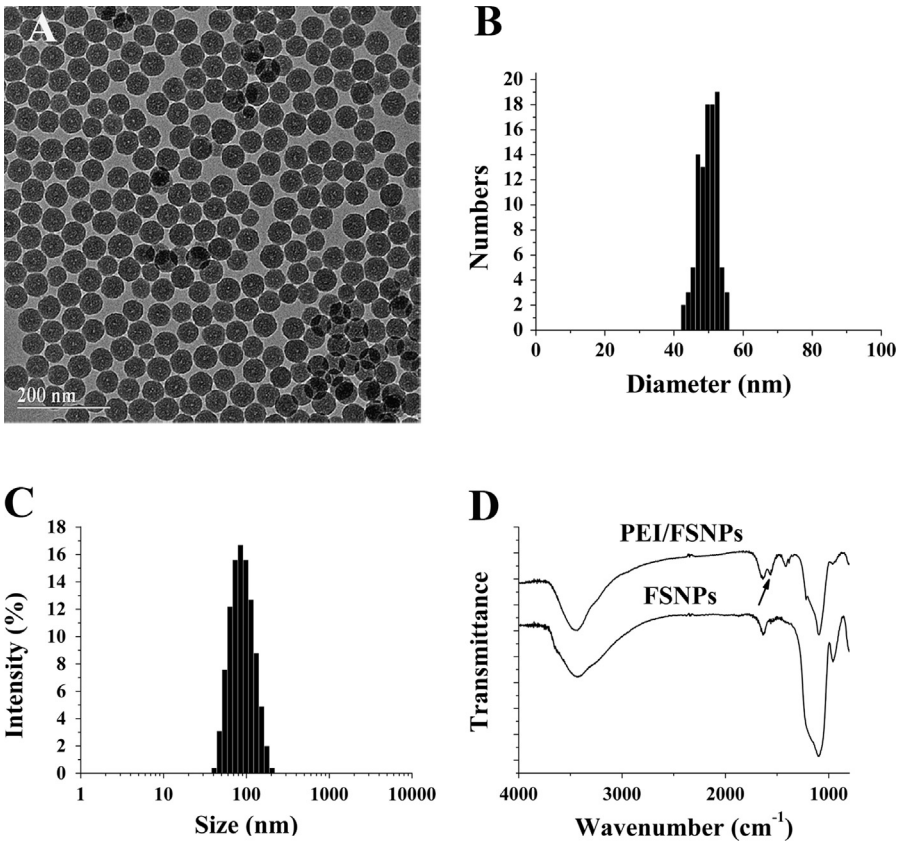

Fig. 2. (A) TEM image of FSNPs (scale bar: 200 nm); (B) histogram of FSNPs' size distribution; (C) DLS of the FSNPs in water; (D) FT-IR spectrum of the PEI/FSNPs and FSNPs composites.

After sonicating the FSNPs in the PEI solution, the surface ζ potential of the nanoparticles was totally reversed to be positive and the hydrodynamic diameter increased to 114.8 nm when dispersed in water (Fig. S2). The FT-IR spectrum of the PEI/FSNPs displayed absorption peak at 1569 cm^{-1}, which was assigned to the N–H asymmetric bending vibration. In contrast, the FSNPs didn't show obvious absorption peak in this wavenumber (Fig. 2D). Both the ζ-potential and IR spectra confirmed that PEI molecules were adsorbed onto the FSNPs successfully.

The adsorbed content of PEI on FSNPs was estimated by thermogravimetric analyses (TGA). After heating to 800 °C, FSNPs and PEI/FSNPs had a weight loss of 18.6 wt% and 25.6 wt%, respectively (Fig. S3). Which meant the content of the adsorbed PEI was 7.0 wt%.

Before biological experiments, PEI/FSNPs' particle size and ζ-potential were measured in three solutions (PBS, DMEM cell culture media and DMEM supplemented with 10% fetal calf serum, respectively). We observed that the addition of protein leads to improved particle dispersion (Fig. S4A), because the protein adsorbed onto the PEI/FSNPs' surfaces reduced the colloidal forces that rendered particle aggregation in salt containing media [56]. While PEI/FSNPs showed a positive charge in water, their ζ-potentials turned negative after dispersion in the above buffer solutions (Fig. S4B).

3.2. ASOs binding affinities toward PEI/FSNPs composites and evaluation of the silence effect by Western blots

The FSNPs were highly positive charged by coating PEI, which facilitated the subsequent combination between the PEI/FSNPs and the ASOs. To investigate the ASOs loading capability on PEI/FSNPs, agarose gel electrophoreses were performed and the results were shown in Fig. 3A. In comparison with the free ASOs as control, the ASOs were completely retarded when the weight ratio of PEI/FSNPs to ASOs reached 30:1 in lane 3. To optimize the weight ratio of PEI/FSNPs to ASOs, we monitored the dynamic light scattering and ζ-potential changes of the mixture solutions at the same time. When the weight ratios decreased from 75:1 to 15:1, the particle size increased from 110.3 nm to 1361 nm gradually. But when the weight ratio decreased to 10:1, the particle size suddenly dropped to 133.6 nm. This phenomenon was ascribed to the ζ-potential changes on the nanoparticle surfaces. At first, the ζ-potential decreased correspondingly with the weight ratio, until the weight ratio reached 15:1 where the ζ-potential was almost 0 mV and the aggregates formed. Further decrease of the weight ratio led to a negative ζ-potential and as a result, the agglomerated particles were re-dispersed.

The cytotoxicity of PEI/FSNPs was investigated by means of a methyl thiazolyl tetrazolium (MTT) assay and no obvious cytotoxic effect was observed (Fig. S5), which was in consistent with the former report [44], indicating that the synthesized PEI/FSNPs were relatively biocompatible and suitable as carriers. The stability of PEI/FSNPs during cellular uptake was confirmed by coating FSNPs with rhodamine B-labeled PEI. Confocal microscopy shown that both labels co-localized in the cells even after 24 h incubation (Fig. S6).

The silence efficiency by ASOs/PEI/FSNPs composites was confirmed by the decreased expression measurements of survivin protein, as demonstrated by the Western blot (Fig. 3B). After delivery of survivin ASOs by PEI/FSNPs composites into HeLa cells, through evaluation in comparison with the PEI/FSNPs composites treated cells, a 40% knockdown efficiency was obtained when the concentration of the survivin ASOs was 500 nM. When the concentration of survivin ASOs was 200 nM, 20% knockdown efficiency was realized. The silence experiments confirmed that our PEI/FSNPs were able to delivery ASOs and reduce the survivin's expression in HeLa cells successfully.

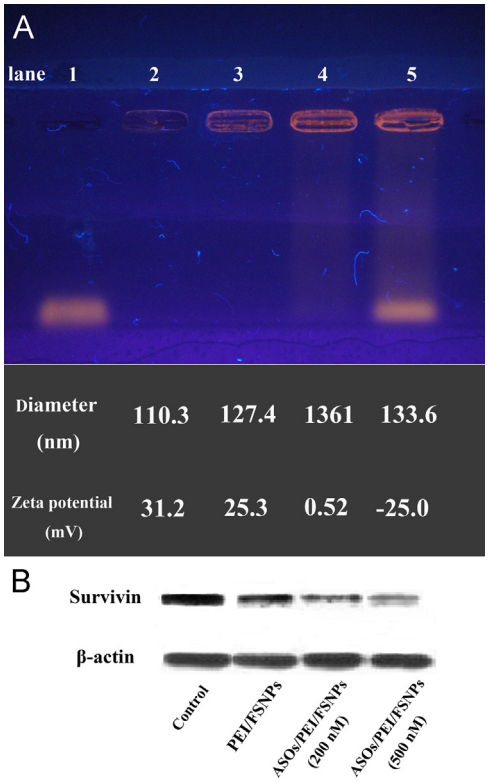

Fig. 3. (A) Agarose retardation results (lane 1: survivin ASOs as control, the weight ratios of PEI/FSNPs to ASOs-TAMAR from lane 2 to lane 5 are 75:1, 30:1, 15:1 and 10:1, respectively, and the corresponding final concentration of ASOs-TAMAR from lane 2 to lane 5 are 25 μM, 35.7 μM, 41.7 μM and 44.1 μM, respectively) and DLS/Zeta potentials of ASOs/PEI/FSNPs composites (each value responses to the sample from lane 2 to lane 5). (B) The Western blot experiment shows that survivin expression has been silenced in HeLa cells after transfected by ASOs/PEI/FSNPs composites for 48 h. The β-actin here was used as reference.

3.3. Preliminary studies on tracking ASOs/PEI/FSNPs composites

The cellular uptake and intracellular transport of ASOs/PEI/FSNPs composites are important for efficient gene delivery. The transport ability of PEI/FSNPs was investigated first. The cell nucleus was stained with DAPI, so the control sample only showed blue luminescence in Fig. 4A. After uptaken by HeLa cells, the ASOs-TAMAR/PEI/FSNPs composites exhibited green luminescence of FITC and red luminescence of TAMAR respectively under CLSM, and the merged image showed yellow emission in the cytoplasm (Fig. 4B). On the contrary, no obvious luminescence was observed in the cytoplasm for cells treated with the same concentration of free survivin ASOs-TAMAR (Fig. 4C). The results proved that the survivin ASOs could not be transported into the cytoplasm without the help of PEI/FSNPs. Flow cytometry was used to quantify the internalized survivin ASOs. Here, we used FAM labelled survivin ASOs and PEI/SNPs, because our flow cytometer only has one excitation laser at 488 nm. As shown in Fig. 4D, ASOs-FAM/PEI/SNPs incubated cells have much higher luminescence intensities compared with ASOs-FAM incubated and control cells.

3.4. Preliminary studies on cellular uptake mechanism of ASOs/PEI/FSNPs composites

Positively charged gene vectors have been used widely in gene transfection. Many researchers thought the main reasons for the

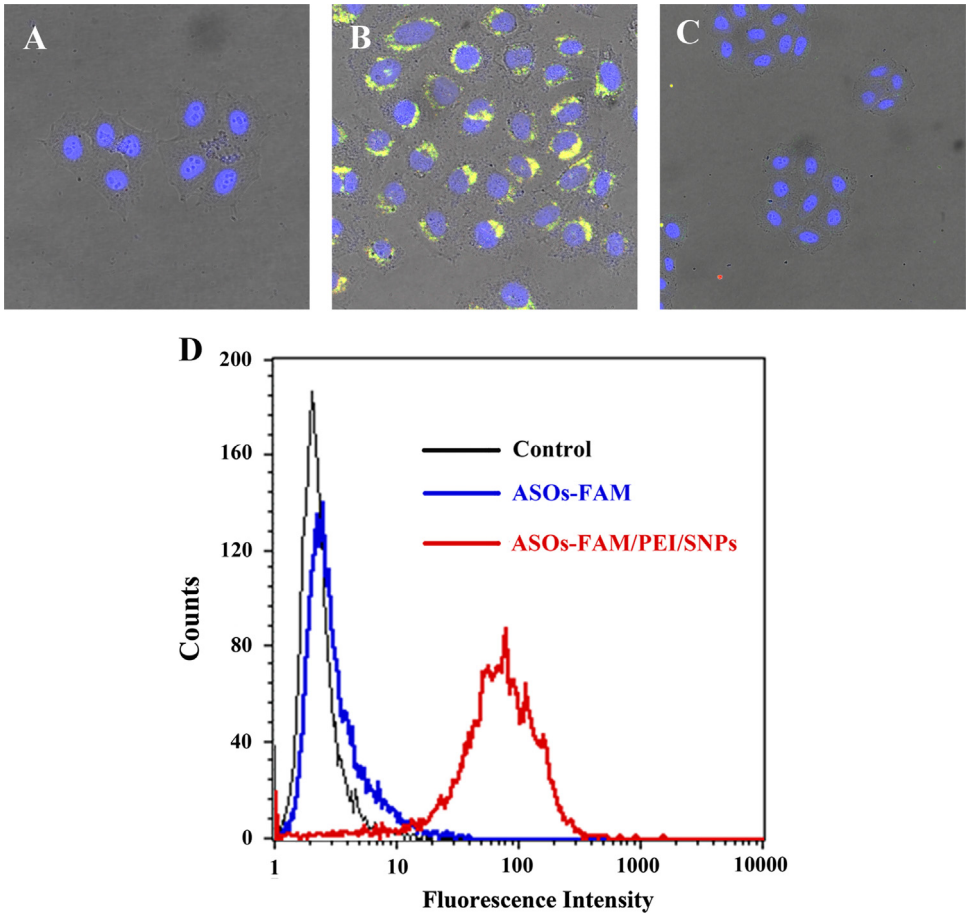

Fig. 4. Confocal microscopy images of (A) control, (B) ASOs-TAMAR/PEI/FSNPs composites. The cell nuclei are stained blue (DAPI), The yellow is the result of the overlap of green (PEI/FSNPs composites) and red (survivin ASOs-TAMAR), (C) survivin ASOs-TAMAR, (D) Flow cytometry analyses on the control (black), survivin ASOs-FAM (blue) and ASOs-FAM/PEI/SNPs composites (red). [PEI/FSNPs]=40 μg/mL, [ASOs]=100 nM. Incubation time: 12 h. (For interpretation of the references to color in this figure legend, the reader is referred to the web version of this article.)

enhanced cellular uptake were due to the electrostatic attraction based on the fact that the cell membranes were negatively charged. But in fact, when the positively charged gene vectors were mixed with culture medium, especially in fetal calf serum (FCS), the ζ-potential dropped to negative values, which meant during the whole transfection process, electrostatic force was no longer a main motive power. The uptake mechanism was also investigated by many researchers, but it was still unclear [57,58]. Therefore, it is interesting to find out the uptake mechanism for our ASOs/PEI/FSNPs composites. As we know, at low temperature, the adenosine triphosphate (ATP) produced by cells will reduced, and inhibited the endocytosis process, so we performed a set of control experiments by incubating ASOs/PEI/FSNPs composites with HeLa cells at 4 °C and 37 °C, respectively. Very weak luminescence was detected in the cells cultured at 4 °C in comparison with the cells cultured at 37 °C (Fig. S7A and B). The result was further quantitatively confirmed using flow cytometry (Fig. S7C), which proved that the cellular uptake of positively charged ASOs/PEI/FSNPs composites was an energy-dependent endocytosis.

3.5. *Intracellular tracking of survivin antisense delivered by PEI/FSNPs composites*

For further understanding where the survivin antisense exerted its function, the intracellular location of ASOs-TAMAR/PEI/FSNPs composites in a single cell was investigated by CLSM using line-plots fluorescent microscopy [59], which presented the information about the spatial distribution of the ASOs-TAMAR/PEI/FSNPs inside HeLa cells. As shown in Fig. 5, quantification of the luminescence intensity profile of ASOs-TAMAR/PEI/FSNPs treated HeLa cells revealed that most of the composites located in the perinuclear regions. *Z*-axis fluorescent microscopy (Fig. 6 and Video S1) further confirmed the position of the composites [60]. As we known, down-regulation of mRNA by ASOs is mainly attributed to the activation of endogenous RNase *H* after ASOs' binding to their targeted mRNA. RNase *H* is an important part of RNA-induced silencing complex (RISC), and it is in charge of cleaving mRNA. Recent reports also indicated that the RISC was located in perinuclear regions [61,62]. Therefore, it can be deduced that the perinuclear region is the location where antisense regulation process takes place.

3.6. *in situ tracking of ASOs/PEI/FSNPs composites into cells*

The intracellular behaviors of ASOs/PEI/FSNPs composites, including uptake and transport, were monitored in real time by the time-lapse confocal microscopy. At first in Fig. 7, nearly no composites were attached to cell surface, because the composites surface had negative potential when they were mixed with DMEM containing 10% FCS. Subsequent incubation over a period of 4 h allowed the composites to enter and accumulate inside cells, suggesting efficient transport across the plasma membrane. It was interesting that at 12 h, we observed cells' mitosis, and the cells became round. At 14 h, when one cell divided into two cells, the composites inside were also separated (Video S2, single channel images in Fig. S8). In the earlier studies, there were few

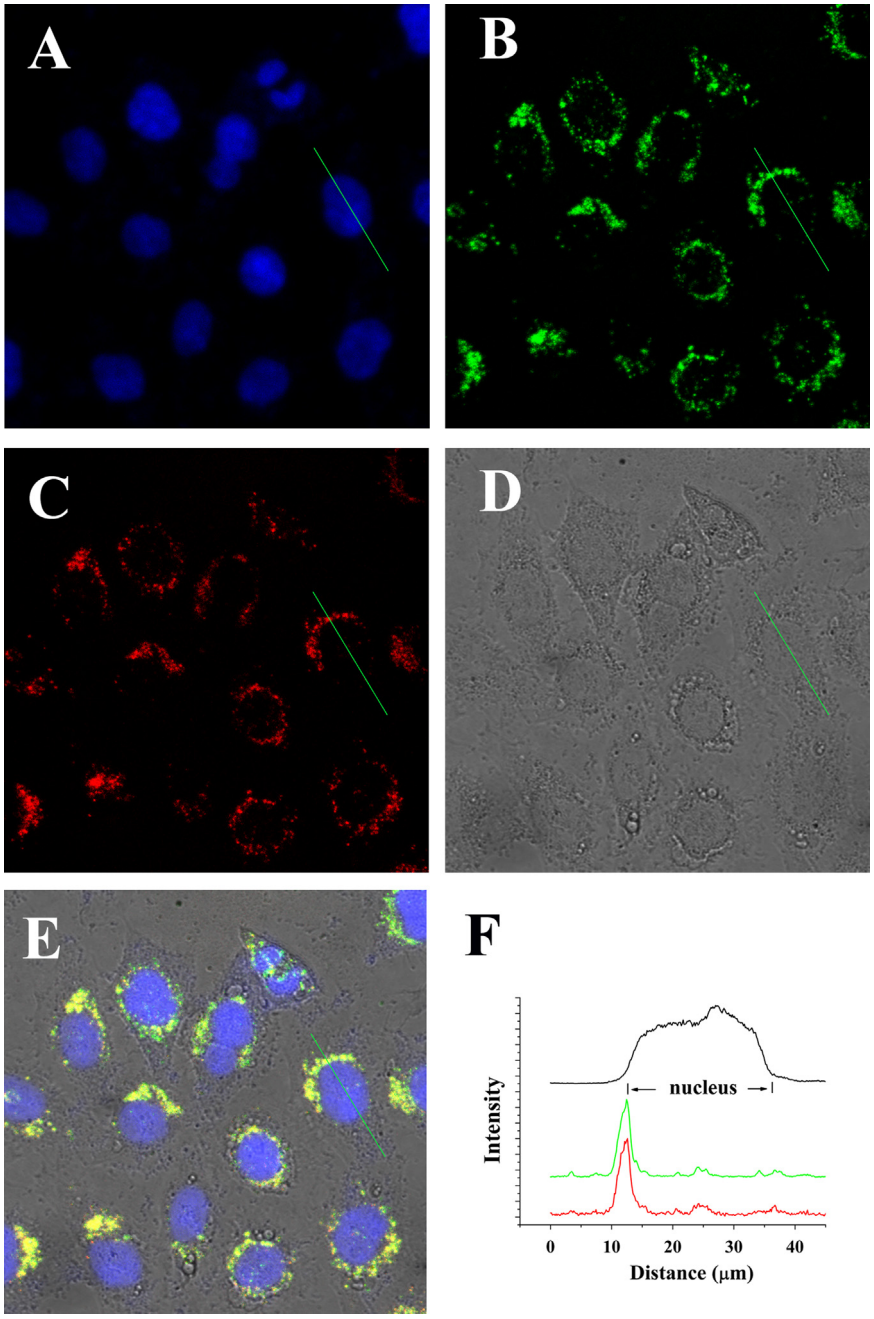

Fig. 5. Confocal fluorescence images of living HeLa cells incubated with ASOs-TAMAR/PEI/FSNPs composites at 37 °C.(A) nucleus fluorescence images; (B) FSNPs fluorescence images; (C) ASOs-TAMAR fluorescence images; (D) bright field images; (E) merged images; (F) Luminescence intensity profile across the line shown in confocal fluorescence images. [PEI/FSNPs]=40 μg/mL, [ASOs]=100 nM.

reports concerned about where the transfected ASOs located after long-time incubation, whether they would be ejected or still be kept inside the next generation cells. Here, we discovered that the transfected ASOs could be delivered from the last generation to the younger generation, which meant their abilities to depress survivin proteins' expression were relative stable and effective even after the mitosis processes.

4. Conclusion

In summary, we have successfully developed a nanocomposite-based ASOs delivery system. Western blot experiment demonstrated that the ASOs adsorbed on the surface of the PEI/FSNPs could specifically induce the down-regulation of the survivin protein's expression. Further systematic investigations revealed that the cellular uptake of the ASOs/PEI/FSNPs composites was an energy dependent process and the perinuclear region was the location where ASOs regulation process took place. In comparison with those previously reported nanocomposite-based ASOs delivery systems, our system has two advantages. On one hand, PEI/FSNPs shows little cytotoxicity even at high concentrations, which means more ASOs can be delivered to cells to achieve better silencing effects. On the other, owing to the fluorescence of the FSNPs, the intracellular localization of the ASOs/PEI/FSNPs composites can be visualized in situ by means of CLSM. As a result, a better understanding of how

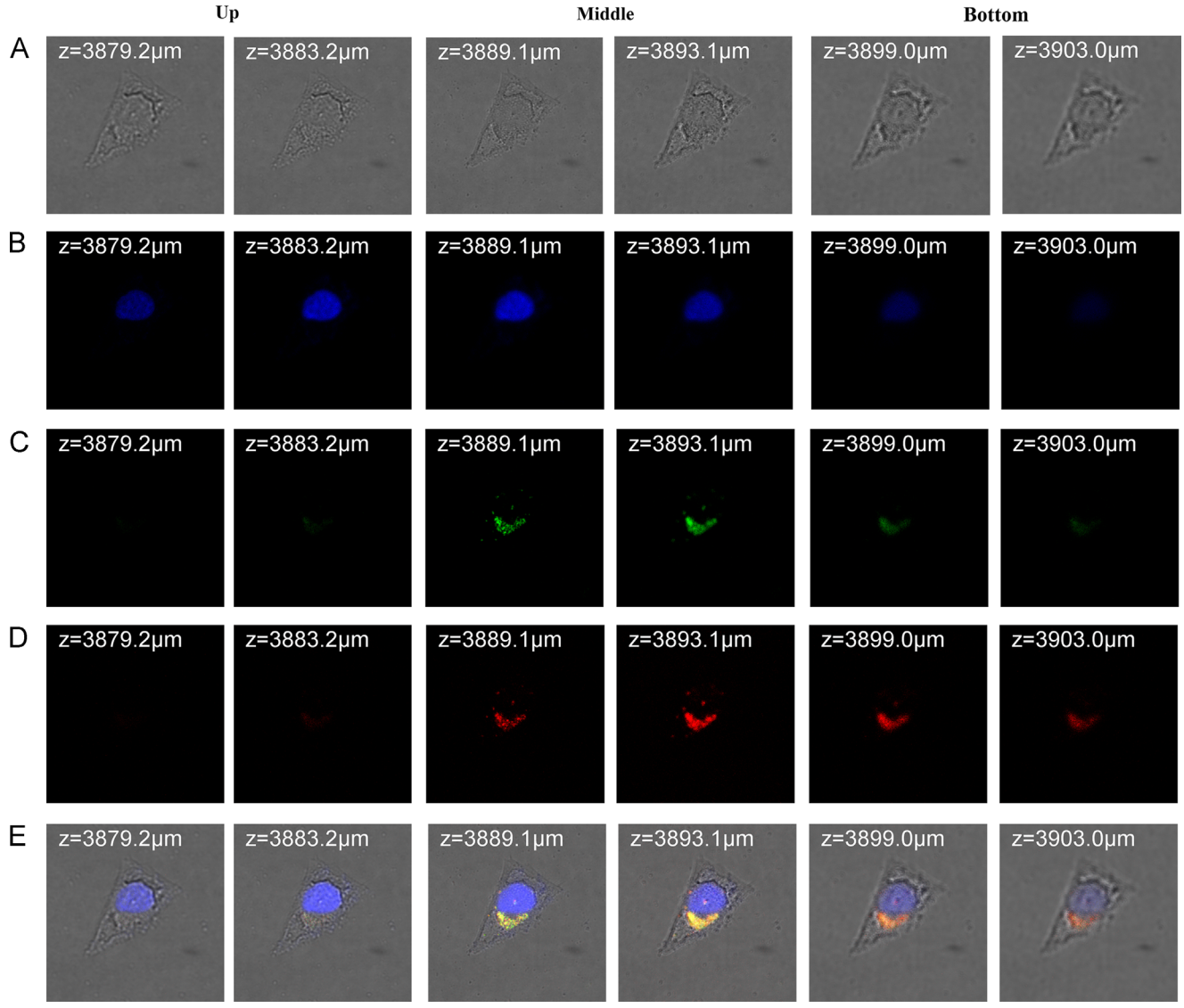

Fig. 6. *Z*-axis confocal images of ASOs-TAMAR/PEI/FSNPs composites uptaken by HeLa cells. (A) bright field; (B) blue channel (nucleus); (C) green channel (PEI/FSNPs); (D) red channel (ASOs-TAMAR); (E) merged picture of the above four channels. (For interpretation of the references to color in this figure legend, the reader is referred to the web version of this article.)

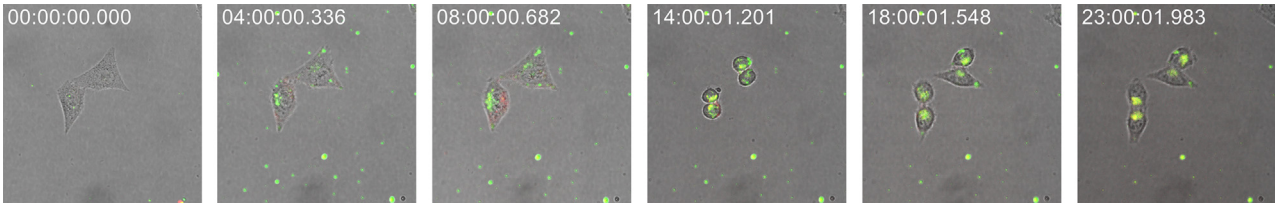

Fig. 7. Real time images of ASOs-TAMAR/PEI/FSNPs composites uptaken by HeLa cells under CLSM. [PEI/FSNPs]=40 μg/mL, [ASOs]=100 nM.

PEI/FSNPs composites transported ASOs into cells is achieved, which provides references for designing new promising SNPs-based vectors for gene therapies.

Acknowledgement

This work was supported by National Basic Research Program of China (2013CB934101), the National Natural Science Foundation of China (21175029, 21271045), Key project (v200801) from Ministry of Education of China, Shanghai Leading Academic Discipline Project (B109) and the NCET-11-0115.

Appendix A. Supplementary material

Supplementary data associated with this article can be found in the online version at http://dx.doi.org/10.1016/j.talanta.2014.03.045.

References

[1] R.A. Stahel, U. Zangemeister-Wittke, Lung Cancer 41 (2003) 81–88.
[2] N.M. Dean, C.F. Bennett, Oncogene 22 (2003) 9087–9096.
[3] A. Biroccio, C. Leonetti, G. Zupi, Oncogene 22 (2003) 6579–6588.
[4] P.C. Zamecnik, M.L. Stephenson, Proc. Nat. Acad. Sci. U.S.A 75 (1978) 280–284.

[5] L.A. Yakubov, E.A. Deeva, V.F. Zarytova, E.M. Ivanova, A.S. Ryte, L.V. Yurchenko, V.V. Vlassov, Proc. Nat. Acad. Sci. U.S.A 86 (1989) 6454–6458.
[6] S.L. Loke, C.A. Stein, X.H. Zhang, K. Mori, M. Nakanishi, C. Subasinghe, J. S. Cohen, L.M. Neckers, Proc. Nat. Acad. Sci. U.S.A 86 (1989) 3474–3478.
[7] I.M. Verma, N. Somia, Nature 389 (1997) 239–242.
[8] E. Marshall, Science 286 (1999) 2244–2245.
[9] D. Deshpande, P. Blezinger, R. Pillai, J. Duguid, B. Freimark, A. Rolland, Pharm. Res. 15 (1998) 1340–1347.
[10] A. Pathak, S. Patnaik, K.C. Gupta, Biotech. J. 4 (2009) 1559–1572.
[11] D. Reischl, A. Zimmer, Nanomed. Nanotechnol. Biol. Med. 5 (2009) 8–20.
[12] B. Ozpolat, A.K. Sood, G. Lopez-Berestein, J. Intern. Med. 267 (2010) 44–53.
[13] Y.R. Wu, J.A. Phillips, H.P. Liu, R.H. Yang, W.H. Tan, ACS Nano 2 (2008) 2023–2028.
[14] C.H. Lu, C.L. Zhu, J. Li, J.J. Liu, X. Chen, H.H. Yang, Chem. Commun. 46 (2010) 3116–3118.
[15] D.R. Radu, C.Y. Lai, K. Jeftinija, E.W. Rowe, S. Jeftinija, V.S.Y. Lin, J. Am. Chem. Soc. 126 (2004) 13216–13217.
[16] K.K. Sandhu, C.M. McIntosh, J.M. Simard, S.W. Smith, V.M. Rotello, Bioconjug. Chem. 13 (2002) 3–6.
[17] M. Thomas, A.M. Klibanov, Proc. Nat. Acad. Sci. U.S.A. 100 (2003) 9138–9143.
[18] N.L. Rosi, D.A. Giljohann, C.S. Thaxton, A.K.R. Lytton-Jean, M.S. Han, C. A. Mirkin, Science 312 (2006) 1027–1030.
[19] D.A. Giljohann, D.S. Seferos, A.E. Prigodich, P.C. Patel, C.A. Mirkin, J. Am. Chem. Soc. 131 (2009) 2072–2073.
[20] L. Qi, X. Gao, ACS Nano 2 (2008) 1403–1410.
[21] M.V. Yezhelyev, L. Qi, R.M. O'Regan, S. Nie, X. Gao, J. Am. Chem. Soc. 130 (2008) 9006–9012.
[22] J. Jung, A. Solanki, K.A. Memoli, K.-i. Kamei, H. Kim, M.A. Drahl, L.J. Williams, H.-R. Tseng, K. Lee, Angew. Chem. Int. Ed. 49 (2010) 103–107.
[23] D. Pantarotto, R. Singh, D. McCarthy, M. Erhardt, J.P. Briand, M. Prato, K. Kostarelos, A. Bianco, Angew. Chem. Int. Ed. 43 (2004) 5242–5246.
[24] D. Cai, J.M. Mataraza, Z.H. Qin, Z.P. Huang, J.Y. Huang, T.C. Chiles, D. Carnahan, K. Kempa, Z.F. Ren, Nat. Methods 2 (2005) 449–454.
[25] N.W.S. Kam, Z. Liu, H.J. Dai, J. Am. Chem. Soc. 127 (2005) 12492–12493.
[26] Y. Liu, D.C. Wu, W.D. Zhang, X. Jiang, C.B. He, T.S. Chung, S.H. Goh, K.W. Leong, Angew. Chem. Int. Ed. 44 (2005) 4782–4785.
[27] Z. Liu, M. Winters, M. Holodniy, H. Dai, Angew. Chem. Int. Ed. 46 (2007) 2023–2027.
[28] A. Vanblaaderen, A. Vrij, J. Colloid Interface Sci. 156 (1993) 1–18.
[29] A. Vanblaaderen, A. Vrij, Langmuir 8 (1992) 2921–2931.
[30] W. Stöber, A. Fink, E. Bohn, J. Colloid Interface Sci. 26 (1968) 62–69.
[31] M. Qhobosheane, S. Santra, P. Zhang, W.H. Tan, Analyst 126 (2001) 1274–1278.
[32] S. Santra, K.M. Wang, R. Tapec, W.H. Tan, J. Biomed. Opt. 6 (2001) 160–166.
[33] S. Santra, P. Zhang, K.M. Wang, R. Tapec, W.H. Tan, Anal. Chem. 73 (2001) 4988–4993.
[34] F.J. Arriagada, K. Osseo-Asare, J. Colloid Interface Sci. 211 (1999) 210–220.
[35] X.J. Zhao, R.P. Bagwe, W.H. Tan, Adv. Mater. 16 (2004) 173.
[36] X.J. Zhao, R. Tapec-Dytioco, W.H. Tan, J. Am. Chem. Soc. 125 (2003) 11474–11475.
[37] L. Wang, C. Lofton, M. Popp, W. Tan, Bioconjug. Chem. 18 (2007) 610–613.
[38] S. Santra, H. Yang, D. Dutta, J.T. Stanley, P.H. Holloway, W.H. Tan, B.M. Moudgil, R.A. Mericle, Chem. Commun. (2004) 2810–2811.
[39] S. Santra, B. Liesenfeld, D. Dutta, D. Chatel, C.D. Batich, W.H. Tan, B.M. Moudgil, R.A. Mericle, J. Nanosci. Nanotechnol. 5 (2005) 899–904.
[40] H. Shi, X. He, Y. Yuan, K. Wang, D. Liu, Anal. Chem. 82 (2010) 2213–2220.
[41] C. Kneuer, M. Sameti, U. Bakowsky, T. Schiestel, H. Schirra, H. Schmidt, C. M. Lehr, Bioconjug. Chem. 11 (2000) 926–932.
[42] X.X. He, K.M. Wang, W.H. Tan, B. Liu, X. Lin, C.M. He, D. Li, S.S. Huang, J. Li, J. Am. Chem. Soc. 125 (2003) 7168–7169.
[43] D.J. Bharali, I. Klejbor, E.K. Stachowiak, P. Dutta, I. Roy, N. Kaur, E.J. Bergey, P. N. Prasad, M.K. Stachowiak, Proc. Nat. Acad. Sci. U.S.A 102 (2005) 11539–11544.
[44] J.E. Fuller, G.T. Zugates, L.S. Ferreira, H.S. Ow, N.N. Nguyen, U.B. Wiesner, R. S. Langer, Biomaterials 29 (2008) 1526–1532.
[45] W.-T. He, Y.-N. Xue, N. Peng, W.-M. Liu, R.-X. Zhuo, S.-W. Huang, J. Mater. Chem. 21 (2011) 10496–10503.
[46] H. Lee, D. Sung, M. Veerapandian, K. Yun, S.-W. Seo, Anal. Bioanal. Chem. 400 (2011) 535–545.
[47] S.G. Zhu, J.J. Xiang, X.L. Li, S.R. Shen, H.B. Lu, J. Zhou, W. Xiong, B.C. Zhang, X. M. Nie, M. Zhou, K. Tang, G.Y. Li, Biotechnol. Appl. Biochem. 39 (2004) 179–187.
[48] Z. Li, S.G. Zhu, K. Gan, Q.H. Zhang, Z.Y. Zeng, Y.H. Zhou, H.Y. Liu, W. Xiong, X. L. Li, G.Y. Li, J. Nanosci. Nanotechnol. 5 (2005) 1199–1203.
[49] Y. Yamazaki, M. Nango, M. Matsuura, Y. Hasegawa, M. Hasegawa, N. Oku, Gene Ther. 7 (2000) 1148–1155.
[50] M. Neu, D. Fischer, T. Kissel, J. Gene Med. 7 (2005) 992–1009.
[51] H. Duan, S. Nie, J. Am. Chem. Soc. 129 (2007) 3333–3338.
[52] B.M. Ryan, N. O'Donovan, M.J. Duffy, Cancer Treat. Rev. 35 (2009) 553–562.
[53] J. Peng, X. He, K. Wang, W. Tan, H. Li, X. Xing, Y. Wang, Nanomed. Nanotechnol. Biol. Med. 2 (2006) 113–120.
[54] Y.L. Li, X. Duan, L.H. Jing, C.H. Yang, R.R. Qiao, M.Y. Gao, Biomaterials 32 (2011) 1923–1931.
[55] T.A. Xia, M. Kovochich, M. Liong, H. Meng, S. Kabehie, S. George, J.I. Zink, A. E. Nel, ACS Nano 3 (2009) 3273–3286.
[56] A. Elbakry, A. Zaky, R. Liebkl, R. Rachel, A. Goepferich, M. Breunig, Nano Lett. 9 (2009) 2059–2064.
[57] T.H. Chung, S.H. Wu, M. Yao, C.W. Lu, Y.S. Lin, Y. Hung, C.Y. Mou, Y.C. Chen, D. M. Huang, Biomaterials 28 (2007) 2959–2966.
[58] D. Pantarotto, J.P. Briand, M. Prato, A. Bianco, Chem. Commun. (2004) 16–17.
[59] C.Y. Li, M.X. Yu, Y. Sun, Y.Q. Wu, C.H. Huang, F.Y. Li, J. Am. Chem. Soc. 133 (2011) 11231–11239.
[60] M.Y. Wang, S.N. Yu, C.A. Wang, J.L. Kong, ACS Nano 4 (2010) 6483–6490.
[61] J.D. Liu, M.A. Valencia-Sanchez, G.J. Hannon, R. Parker, Nat. Cell Biol. 7 (2005) 719–723.
[62] G.L. Sen, H.M. Blau, Nat. Cell Biol. 7 (2005) 633–636.